Lab on a Chip

Accepted Manuscript

ROYAL SOCIETY OF CHEMISTRY

www.rsc.org/loc

University at Buffalo
The State University of New York
Department of Electrical Engineering
School of Engineering and Applied Sciences

Graphical Entry

Text

This article provides a comprehensive overview of the physics of the gas solubility and permeability of PDMS, a systematic review of different types of the vacuum-driven power-free microfluidics, design guidelines, existing applications, and the outlook.

Image

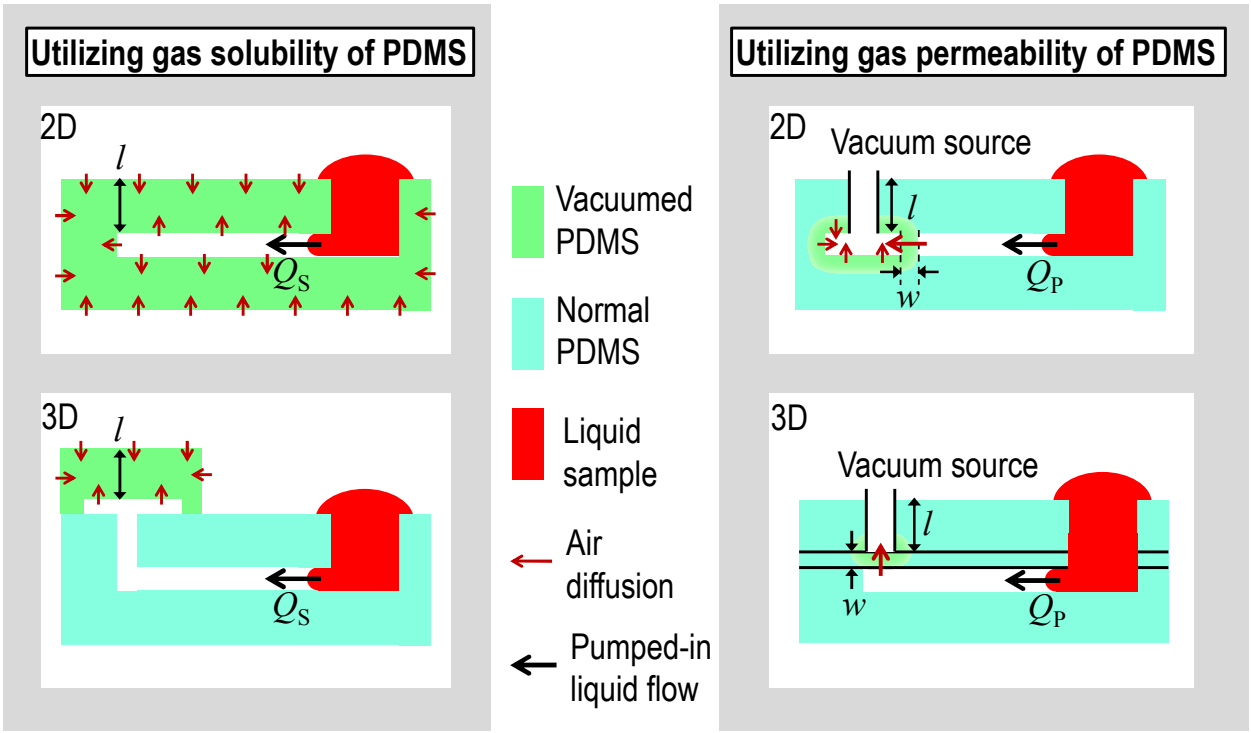

Lab on a Chip

CRITICAL REVIEW

Vacuum-driven power-free microfluidics utilizing the gas solubility or permeability of polydimethylsiloxane (PDMS)

Received 00th January 20xx,
Accepted 00th January 20xx

DOI: 10.1039/x0xx00000x

www.rsc.org/

Linfeng Xu,[a,b] Hun Lee,[a,c] Deekshitha Jetta[a] and Kwang W. Oh[a]*

Suitable pumping methods for flow control remain a major technical hurdle in the path of biomedical microfluidic systems for point-of-care (POC) diagnostics. Vacuum-driven power-free micropumping method provides a promising solution to such a challenge. In this review, we focus on vacuum-driven power-free microfluidics based on the gas solubility or permeability of polydimethylsiloxane (PDMS); degassed PDMS can restore air inside it due to its high gas solubility or gas permeable nature of PDMS can allow the transfer of air into a vacuum through it due to its high gas permeability. Therefore, it is possible to store or transfer air into or through the gas soluble or permeable PDMS, in order to withdraw liquids into the embedded dead-end microfluidic channels. This article critically overviews a comprehensive look at the physics of the gas solubility and permeability of PDMS, a systematic review of different types of the vacuum-driven power-free microfluidics, guidelines for designing solubility-based or permeability-based PDMS devices, alongside existing applications. Advanced topics and the outlook in using the micropumping utilizing the gas solubility or permeability of PDMS will be also discussed. We stronlgy recemmend that microfluidics and lab-on-chip (LOC) communities harness vacuum energy to develop smart vacuum-driven microfluidic systems.

1. Introduction

With the coming age of point-of-care (POC) diagnostics, microfluidics seems have its most promising opportunities because numerous of stringent requirements in POC diagnostics, such as portability, low cost per test, small amount of sample and short sample processing time, can be fulfilled by microfluidic devices.[1-6] However, despite all the recent advances made in the microfluidic fields, flow control still remains a major technical hurdle in the path of microfluidic systems particularly for POC diagnostics.[1, 7-11]

Linfeng Xu *received his MS and PhD degrees in electrical engineering from University at Buffalo, State University of New York in 2011 and 2014 respectively in Kwang W. Oh's SMALL lab. His current research interests include design, fabrication and analysis of MEMS/NEMS, generation and manipulation of microdroplets, microfluidics for point-of-care blood separation & test, micromagnectic particles based immunoassay and single cell electroporation by nanofountain probes.*

Hun Lee *received his BS and MS degrees in electrical engineering from Dankook University, Korea in 2007 and 2009, respectively. He subsequently received his PhD in electrical engineering at SUNY at Buffalo in 2015 in Kwang W. Oh's SMALL lab. He is currently at SK Hynix, Korea. His research interests include design and analysis of droplet-based microfluidic systems using magnetic particles and microfabrication technology.*

Deekshitha Jetta *graduated from Jawaharlal Nehru Technological University, India in 2012 with bachelor's degree in electronics and communication engineering before pursuing her MS degree in electrical engineering at SUNY at Buffalo in 2015. She is currently pursuing her PhD in electrical engineering at SUNY at Buffalo in Kwang W. Oh's SMALL lab. Her research interests include microfluidic systems for point-of-care diagnostics, blood based diagnostics, nano-electronics and nano-photonics.*

[a] SMALL (Sensors and MicroActuators Learning Laboratory), Department of Electrical Engineering, State University of New York at Buffalo, Buffalo, NY, 14260, USA; E-mail: kwangoh@buffalo.edu.
[b] Current address: Intuitive Biosciences, 8137 Forsythia St., Suite 138, Middleton, WI 53562, USA.
[c] Current address: SK Hynix, 2091 Gyeongchung-daero, Bubal-eub, Icheon-si, Gyeonggi-do, S. KOREA.

Currently most of the flow control methods for POC microfluidic systems either focus on the ease of usage and low energy consumption or 'wall free' approaches, which include capillary flow,[12] evaporation,[12] droplet-based passive pumping,[13] gravity-driven flow[14, 15] and finger squeeze-driven flow,[16] thereby neglecting the abilities to generate constant and well-controlled flow. In general, in order to achieve a better control of the flow, active pumping methods with complicated external macro parts, such as pressure and electrokinetic driven pumping are needed, which are usually not very suitable for POC diagnostics. [1-4, 12, 13, 17] This conflict between the simplicity and the precision of flow control has driven microfluidic researchers to come up with better solutions.

One simple and clever approach to the goal was made by the combination of capillary flow with gravity.[18] Through tilting a microfluidic platform, the capillary flow rate could be controlled from 10 to 1000 nL min^{-1}. While the challenges of this method for POC diagnostics are that it is not easy to control the tilting angle without the help of a machine and relatively large volume of liquid is needed to exploit the application of gravity in microfluidic devices.

An even simpler method of flow control in polydimethylsiloxane (PDMS) based microfluidic devices has been proposed by Maeda *et al*.[19] Because of the gas solubility of PDMS, air molecules can be evacuated from a PDMS microfluidic device by keeping it in a vacuum environment for a period of time. As a result, vacuum is stored in the PDMS substrate. Once the device is brought into exposure with atmospheric pressure, flow will be generated in the dead-end microfluidic channels as the trapped air is reabsorbed by the pre-evacuated PDMS substrate. And flow control is possible by adjusting the air evacuation time, although the control is not accurate or linear.[20]

Another approach is to utilize the gas permeable nature of PDMS.[21] It is known that pressurized air can disappear through the gas permeable PDMS membrane due to its high gas permeability, so we can remove trapped air bubbles inside microfluidic channels.[22-24] Likewise, air can diffuse through the PDMS membrane into a vacuum reservoir.[21, 25] Based on Fick's law of diffusion,[26] the penetrant gas will diffuse across the PDMS layer due to the concentration gradient, allowing the liquid filling of dead-end microfluidic channels.

The biggest advantages of these methods utilizing the gas soluble or permeable nature of PDMS are that there is no need of surface treatment when compared with capillary pumping and as long as the microfluidic devices are made of PDMS, no integration of micropumps is needed. These advantages are extremely suitable for POC microfluidic systems, therefore lots of developments and applications based on these pumping methods have been developed since then.[3, 19, 27-30] However, there is no systematic review about the vacuum-driven power-free pumping method utilizing the gas solubility or permeability of PDMS yet. In this paper, we critically review the physics of the gas solubility and permeability of PDMS, different types of the vacuum-driven power-free pumping methods and examples of applications. Limitations and an outlook of the vacuum-driven power-free microfluidics are discussed. In this review, we will not cover common methodologies, such as direct application of a vacuum at a reservoir outlet,[31-33] and vacuum controlled Quake's pneumatic valves.[34, 35] Rather, we will focus on the approaches based on the gas soluble or permeable nature of PDMS. This review article will provide simple and straightforward design strategies for developing POC friendly microfluidic systems and smart vacuum-driven microfluidic applications.

Kwang W. Oh

Kwang W. Oh *is an Associate Professor at SUNY at Buffalo where he leads Sensors and MicroActuators Learning Lab–SMALL (small.buffalo.edu or MicroTAS.org). He received his bachelor's degree in physics from Chonbuk National University, Korea, in 1995. He earned his MS and PhD degrees in electrical and computer engineering from University of Cincinnati in 1997 and 2001, respectively. Prior to joining SUNY at Buffalo, he worked at Samsung Advanced Institute of Technology (SAIT), Korea, where he developed micro PCR and LOC platforms for clinical diagnostics. He has been selected as one of the prestigious Lab on a Chip's 2012 Emerging Investigators. His current research focuses on vacuum-driven power-free microfluidics, pressure-driven microfluidic networks, droplet-based microfluidics, on-chip blood separation, 3D cell culture platforms, noninvasive continuous blood pressure monitoring, micro valves and actuators, and microfluidic applications for high throughput and point-of-care test.*

2. Gas solubility and permeability of PDMS

Over the past two decades, soft lithography is used frequently to make microfluidic devices and PDMS is the most commonly used stamp resin in the procedure of soft lithography.[36-40] The major advantages of using PDMS in microfluidics are:

• **Easy to fabricate**. Before curing, PDMS is in liquid phase which could be easily poured into any mould. After curing at 65 °C for several hours it would turn into rubber-like elastics which are easy to be peeled off from the mould while keeping all the finest patterns of the mould.

• **Relatively inexpensive**. PDMS belongs to a group of polymeric organic silicon compounds that are commonly referred to as silicones which are not difficult to be made.

• **Chemically inert/non-hazardous**. As PDMS is one type of silicones, it has the typical chemical characteristic of silicones which are not active and relatively non-hazardous.

• **Optically clear**. This characteristic of PDMS makes it possible so that we could observe the device structures made by

Table 1 Summary of solubility, diffusivity and permeability parameters in PDMS at 35 °C. From [26]; Copyright Institute of Physics.

Penetrant	Solubility (S) [cm^3 (STP)/(cm^3 · atm)]	Diffusivity (D_0) [cm^2/s]	Permeability (P_0) [Barrer = 10^{-10} cm^3 (STP) · cm/(cm^2 · s · cm Hg)]	m [1/atm]
O_2	0.18 ± 0.01	(34 ± 1) × 10^{-6}	800 ± 20	(-3.4 ± 2.7) × 10^3
N_2	0.09 ± 0.008	(34 ± 1) × 10^{-6}	400 ± 10	(-3.5 ± 3.4) × 10^3
CO_2	n/a	(22 ± 1) × 10^{-6}	3800 ± 70	n/a

PDMS and the process that takes inside the devices directly under microscopes.

• **Flexible and fairly tough when cured**. Because of this characteristic of PDMS, it is easy to handle the microdevices based on PDMS.

• **Gas soluble and permeable**. PDMS could be considered like a liquid even though it is in solid state. It could absorb gas and let gas go through with a liquid-like matrix.[26] Based on this property of PDMS, it is possible to store or transfer vacuum from the degassed PDMS to the embedded dead-end microfluidic channels and withdraw liquids into the microfluidic channels. The kinetics of gas transport through a thin PDMS layer has been studied, and such measurements can yield solubility S [cm^3 (STP)/(cm^3 · atm)], diffusivity D [cm^2/s] and permeability P [Barrer = 10^{-10} cm^3 (STP) · cm/(cm^2 · s · cm Hg)].[26,41] **Table 1** summarizes values associated with solubility, diffusivity and permeability of PDMS to N_2 and O_2 gas at 35 °C.[26, 41, 42] If one assumes the diffusivity to be constant, the relationship between the permeability, the solubility and the diffusivity simplifies to: $P \approx S \times D$. The physics of the gas solubility and permeability of PDMS is described in detail as following.

Gas solubility of PDMS

Pressure dependence of gas solubility in rubbery polymers is typically described using Henry's law. The concentration of soluble gases in PDMS roughly exhibits a linear relationship with the penetrant pressure at a fixed temperature.[26, 41, 42] This sorption isotherm of PDMS can be defined as:

$$S = \frac{C}{p} \tag{1}$$

where S [cm^3 (STP)/(cm^3 · atm)] is the Henry's law constant (or the solubility coefficient), C [cm^3 (STP)/cm^3], with the unit as cm^3 (standard conditions for temperature and pressure, STP) of gas absorbed per cm^3 of PDMS, is the equilibrium gas concentration in the PDMS at pressure p [atm]. It is well studied that N_2 and O_2 sorption in PDMS obey Henry's law over a rather wide pressure range.[41]

For example, the equilibrium concentration of gas dissolved in the PDMS is proportional to the partial pressure of the gas around the PDMS. If we place a PDMS piece in a vacuum desiccator (i.e., $p_0 \approx 10$ kPa = 0.1 atm) for a period of time, it will be degassed. According to **Eqn. (1)**, the equilibrium air concentration in the degassed PDMS is $C_0 = S_{PDMS} \times p_0 = 0.011$ cm^3 (STP)/cm^3, where $S_{PDMS} \approx 0.8 \times S_{N2} + 0.2 \times S_{O2} = 0.11$ cm^3 (STP)/(cm^3 · atm) and $p_0 = 0.1$ atm. When the pre-vacuumed PDMS piece is brought back to the atmosphere (i.e., $p_1 \approx 100$ kPa = 1 atm), the surfaces of PDMS begin to absorb the air (mostly N_2 and O_2) toward the new equilibrium to $C_1 = S_{PDMS} \times p_1 = 0.11$ cm^3 (STP)/cm^3. Therefore, the PDMS can restore the 0.1 cm^3 (STP) of air per cm^3 of PDMS. The degassed PDMS is to the air as the dry sponge is to the water (**Fig. 1A**).

The air transfer is mainly controlled by diffusion in PDMS. By assuming simple boundary conditions: $C(x, 0) = C_0$ at $t = 0$ sec and $C(l, t) = C_1$ at $x = l$, one can calculate the air concentration profile $C(x, t)$ in the degassed PDMS by Fick's second law of diffusion

$$\frac{\partial C}{\partial t} = D\frac{\partial^2 C}{\partial x^2} \tag{2}$$

Then the air flux F at the surface of the degassed PDMS with a thickness of l will be

$$F = D\left.\frac{\partial C}{\partial x}\right|_{x=l} \approx \frac{D_0(C_1 - C_0)}{l}\exp(-t/\tau) \tag{3}$$

$$\text{and} \quad \tau = \frac{4}{\pi^2}\frac{l^2}{D_0} \tag{4}$$

where D is the diffusion coefficient of gas in PDMS, D_0 is the average diffusion coefficient of the gas, and τ is the characteristic time constant. In the simplest scenario, the gas diffusion coefficient D is constant over the concentration range of interest: $D \approx D_0 = D_{N2} = D_{O2} = 34 \times 10^{-6}$ cm^2/s (**Table 1**). This assumption is usually valid for low-sorbing penetrants in rubbery polymers.[26]

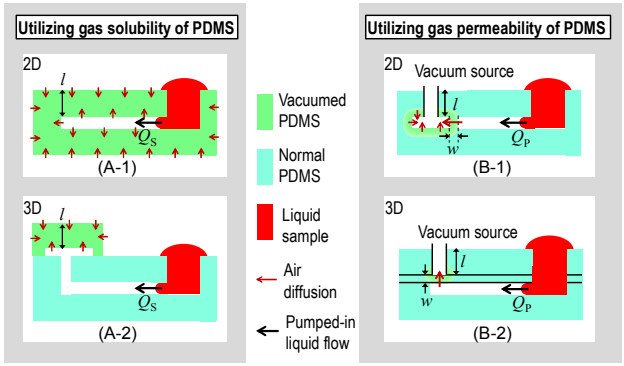

Fig. 1 Vacuum-driven power-free microfluidics utilizing the gas solubility (A) or permeability (B) of PDMS. 2D stands for two-dimensional design and 3D stands for three-dimensional design. l is the thickness of PDMS slab and w is the thickness of the PDMS wall or membrane. Q_S is the solubility-based volumetric flow rate (see Eqn. (7)) and Q_P is the permeability-based volumetric flow rate (see Eqn. (8)).

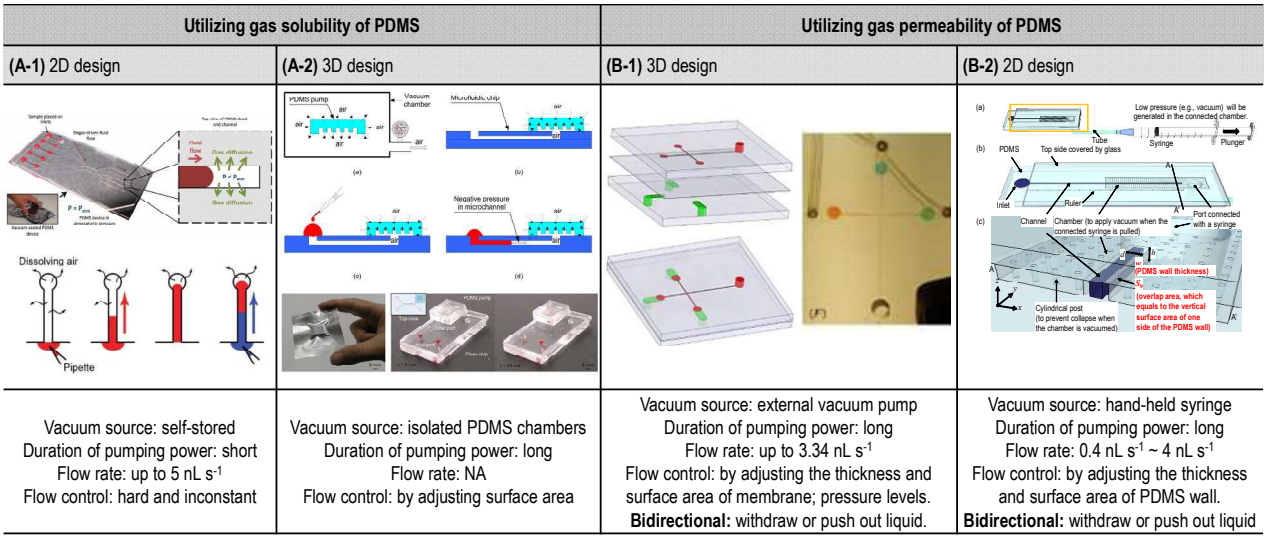

Fig. 2 Different types of vacuum-driven power-free micropumping methods utilizing the gas solubility or permeability of PDMS. **[A]** (A-1) A 2-D design of micropumping utilizing the gas solubility of PDMS. A whole PDMS device is pre-vacuumed in a vacuum environment. See also Fig. 1A. (A-2) A 3-D design of micropumping utilizing the gas solubility of PDMS. A PDMS slab is pre-vacuumed in a vacuum environment. See also Fig. 1A. **[B]** (B-1) A 3-D design of micropumping utilizing the gas permeability of PDMS. External vacuum pumps are connected to the ports in the control channels. See also Fig. 1B. (B-2) A 2-D design of micropumping utilizing the gas permeability of PDMS. An hand-held syringe can generate a vacuum environment. See also Fig. 1B. (A-1) from,[19, 43] copyright Royal Society of Chemistry; (A-2) from,[44] copyright American Institute of Physics; (B-1) from,[21] copyright Institute of Physics; (B-2) from,[25] copyright Springer.

Gas permeability of PDMS

Under the assumption of steady state, the relation between the steady state diffusive flux F [mol/(m^2·s)] and the concentration gradient across a very thin PDMS membrane (w << l) can be described by Fick's law of diffusion

$$F = D\left.\frac{\partial C}{\partial x}\right|_{x=w} \approx D_0 \frac{\Delta C}{w}. \quad (5)$$

In a typical experiment, initially (i.e., at t = 0) the PDMS membrane is at a uniform air concentration, known to be C_1 = 0.11 cm^3 (STP)/cm^3 = 4.89 mol/m^3 at STP.[26, 41, 42] At t > 0, one face of the membrane (at x = w) is exposed to a vacuum (C_{VAC} << C_1), and the other side (at x = 0) is exposed to the atmosphere (~C_{ATM} = 1 cm^3 (STP)/cm^3 = 44 mol/m^3). Therefore, under the assumption of steady state, the steady state air flux of diffusion across the thin PDMS membrane with a thickness of w can be estimated from **Eqn. (5)**. By assuming that amount of air diffused from dead-end microfluidic channels into the PDMS membrane equals to the amount of liquids pumped inside the dead-end microfluidic channels, the volumetric flow rate Q can be calculated when the geometry of the channels is known (**Fig. 1B**).

Another way to understand gas permeability of PDMS is to investigate the dependence of permeability on pressure, which is often described using empirical equations. By assuming diffusion and solubility coefficients to be independent of concentration,[26, 42] from **Eqn. (1)** and **Eqn. (5)**, the steady state gas permeation flux F across a thin PDMS membrane (w) can be described as:

$$F \approx D_0 \frac{\Delta C}{w} = D_0 \frac{S(p_2 - p_1)}{w} = P\frac{\Delta p}{w} \quad (6)$$

where $P = P_0(1 + m\Delta p)$ is the permeability coefficient of that gas, p_2 is the upstream pressure, p_1 is the downstream or permeate pressure, Δp equals $p_2 - p_1$, which is the pressure difference between the upstream and downstream, P_0 is the permeability coefficient at Δp = 0, and m is the characteristic parameter of the pressure dependence of permeability. **Table 1** gives the values of P_0 and m of PDMS for N_2 and O_2.

From **Eqn. (6)**, the gas penetrant flux F can be calculated if the pressure difference Δp is known. Roughly, as one face of the PDMS membrane is in contact with a vacuum and the other face of the PDMS membrane is placed under atmosphere, the pressure difference can be considered as ~1 atm.

3. Micropumping utilizing the gas solubility and permeability of PDMS

As we discussed, the degassed PDMS can restore air in it or the gas permeable PDMS allows the air transfer across the thin membrane. Based on the transport mechanism through the PDMS, there are two types of vacuum-driven power-free microfluidics: (1) the micropumping utilizing the gas solubility of PDMS (**Fig. 1A**) and (2) the micropumping utilizing the gas permeability of PDMS (**Fig. 1B**). In the case of the gas solubility based microfluidics, the PDMS piece itself is used as a self-powered vacuum source. Therefore, the layer thickness could be of the order of several mm (l) with a long characteristic time constant. On the other hand, the permeability based microfluidics requires a very thin membrane of the order

of sub mm (w) for better air transfer with a short characteristic time constant. In each type, based on the structure designs, it can be further divided as two-dimensional (2D) design and three-dimensional (3D) design.

3.1. Micropumping utilizing the gas solubility of PDMS

2D design

Hosokawa *et al*. proposed an original idea of using a PDMS piece as a power-free vacuum source (**Fig. 2A-1**).[19] Because the whole PDMS device was stored in the vacuum desiccator and degassed at 10 kPa for more than 1 hour,[19] the air concentration of PDMS decreased causing the air previously dissolved in the PDMS device to be diffused out of the PDMS piece. Vacuum was pre-stored inside the PDMS substrate. After the PDMS device was taken out of the vacuum chamber and placed under atmosphere, the air concentration in the PDMS piece increased. Therefore, the air trapped in the dead-end microfluidic channels could diffuse back into the pre-vacuumed PDMS piece. The resulting pressure difference drove the sample liquids into the dead-end microfluidic channels. Through different channel designs and controlling the degassing or vacuuming time of the PDMS substrate, flow rates up to 5 nL/s were reported.[19, 20, 27, 28, 30, 45]

As discussed in section 2 (**Eqn. (3)**), the volumetric flow rate Q_S can be calculated by[19]

$$Q_S \propto F\,A(t) = k\frac{A(t)D_0(C_1 - C_0)}{l}\exp(-t/\tau) \quad (7)$$

where k is an empirical factor related to the viscous effect of the pumped-in liquid, the flow hindrance effect of surface tension, and the geometry of the channel, which is usually in inverse proportion to the hydraulic resistance of the microfluidic channel; therefore the volumetric flow rate Q_S can be faster with low-viscosity fluids, short channel lengths, large cross-sectional areas of the channel, and less hydrophobic surfaces. $A(t)$ is the area of the surface where the trapped gas in the dead-end microfluidic channels can diffuse into the PDMS substrate. It is also a function of time as the pumped-in liquid will screen the surface area of the dead-end microfluidic channels. Once the device is placed under atmosphere, its power-free pumping ability will decrease with time exponentially as indicated by **Eqn. (7).**

The advantages of this micropumping method are obvious. Firstly, it is very easy to integrate the micropumping mechanism into microfluidic devices as long as PDMS is used to fabricate the devices. No additional structure or external energy is needed to pump in the flow. Secondly, no surface treatment is needed. Even though the surface is hydrophobic, liquids can still be pumped inside. However, similar to other passive pumping methods, the flow rate is not constant. Once the device is exposed to atmosphere, the pumping rate will decrease with time dramatically. Moreover, in order to employ this type of micropumping method, the device has to be degassed in vacuum environment for more than 1 hour and be sealed in the air-tight package before usage. The users have to finish the test as soon as possible (within ~10 min) once the devices are taken out from the vacuumed packages. This may cause inconvenience and extra cost for POC diagnostics.

3D design

As shown in **Fig. 2A-2**, an isolated PDMS slab was pre-vacuumed and then placed at the outlet of another microfluidic chip to withdraw liquids from inlets.[44] Moreover, in order to increase the pumping time and keep the flow rate constant, the outer surface except the bottom of the isolated PDMS slab was coated with epoxy glue. The volumetric flow rate can be calculated in a similar way as described in **Eqn. (7)**.

The advantages of this method are the concept of 'place-n-play' and the more constant and durable flow rate. Only the isolated PDMS slab needs to be vacuumed. After that, it can be placed on any microfluidic device as an ad-hoc vacuum pump, even though the microfluidic devices are not made of PDMS. In addition, by coating the outer surface of the isolated PDMS slab, more constant and durable flow rate is achieved compared with the pumping by degassing the whole PDMS devices. However, the disadvantage of this method is that the isolated PDMS chamber still needs to be stored in a vacuum environment for a sufficient time and be kept in an air-tight package. To ensure a leak-free seal, the user needs to sturdily press the PDMS slab after placing on the outlet port of the microfluidic device.

3.2. Micropumping utilizing the gas permeability of PDMS

3D design

Instead of pre-degassing the PDMS slab, an external vacuum can be applied through a PDMS membrane (**Fig**. **2B-1**)[21] or a PDMS wall (**Fig. 2B-2**)[25] to the dead-end microfluidic channels. This method is based on the gas permeability of PDMS.

As shown in **Fig. 2B-1**, a vacuum was applied to a control channel, which was separated from the dead-end flow chamber/channel by a thin PDMS membrane at the end.[21] Through controlling the overlap surfaces area between the control channel and the flow chamber/channel, the PDMS membrane thicknesses and vacuum pressure levels, volumetric flow rates Q_P ranging from 0.17 nL/s to 3.34 nL/s were achieved. Moreover, by integrating multiple independent control channels, complicated flow controls such as localized fluid turning at intersections and fluid metering were demonstrated.

Moreover, a much higher flow rate was achieved by utilizing both the gas permeability of PDMS and the capillary effect of glass.[46] As illustrated in **Fig. 3**, the microfluidic channels were made of glass instead of PDMS, consistent flow rates ranging from 1 to 14 μL/min (or 16.67 to 233.34 nL/s) were demonstrated by adjusting control pressures, surface areas and thicknesses of the PDMS membrane.

The advantages of this method are the controllability of pumping rates with various parameters that can regulate the steady-state diffusive air flux F through the PDMS membrane, the longer pumping ability by keeping the constant vacuum level, and the bidirectionality of pumping depending on the polarity of pressure difference (i.e., relatively negative or

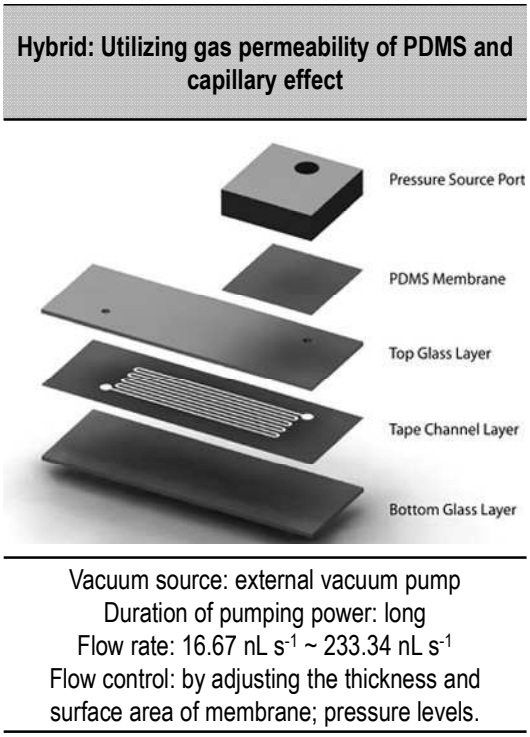

Fig. 3 A hybrid pumping method utilizes gas permeability of PDMS and capillary effect of glass.[46] Copyright Institute of Physics.

positive). However, the disadvantages of this method are that the multiple layers, such as the main flow channels, the control channels, the thin membrane, are required and the external vacuum source should be connected to the control channels.

2D design

As shown in **Fig. 2B-2**, the 3D sandwich structure shown from **Fig. 2B-1** can be simplified to a 2D design. The control channels (*or* pneumatic chambers) are on the same layer with the dead-end microfluidic channels.[25] Recently, Xu *et al*. have demonstrated a volumetric flow rate Q_P ranging from 0.09 to 4 nL/s by controlling the overlap surface areas and the PDMS wall thicknesses between the pneumatic chambers and the dead-end flow channels. They used a manual hand-held syringe to generate an instantaneous vacuum environment. The syringe-assisted vacuum level was well kept for more than 1 hour.

Similar to **Eqn. (7)** for calculating the volumetric flow rate Q_S, here the volumetric flow rate Q_P can be calculated using **Eqn. (5)** by

$$Q_P \propto F\,S(t) = k\,D_0(C_1 - C_0)\frac{S(t)}{w} \qquad (8)$$

where k is an empirical factor related to the viscous effect of the pumped-in liquid, the flow hindrance effect of surface tension, and the geometry of the channel, which is usually in inverse proportion to the hydraulic resistance of the microfluidic channel. $S(t)$ is the total surface area that allows air to diffuse into the PDMS wall (that equals the overlap area of the flow channel and pneumatic chamber), w is the PDMS wall thickness, C_1 and C_0 are the equilibrium air concentrations of the PDMS wall under atmosphere and the vacuum that is applied externally, respectively. In **Eqn. (8)**, we assume that the air concentrations inside the dead-end channel and the pneumatic chamber are unchanged during the pumping process.

Unlike the case of the pre-vacuumed power-free pumping (**section 3.1**), the air flux of diffusion is in the steady state due to the well-maintained vacuum level for a long period of time (i.e., ~1 hr) and the thin PDMS membrane or wall (i.e., $w << l$). Therefore, the volumetric flow rate Q_P can be constant as long as $S(t)$ is kept constant. When the pressure difference completely vanishes inside the pneumatic chamber due to the air diffusion from outside to the chamber, we can re-store the low pressure or vacuum inside the pneumatic chamber by simply reconnecting the syringe and pulling the plunger again. Therefore, unlike the solubility based pumping method, the syringe-assisted method enables instantaneous, recurring, and point-of-care pumping. Another advantage of this method is that the pumping is bidirectional between the dead-end channel and pneumatic chamber. By applying a positive pressure, air bubbles can be injected into the dead-end channel. Thereafter, the drawn-in liquid can be retrieved from the dead-end channel. However, the disadvantage of this approach is that the external vacuum source is still required, although a simple module-type vacuum source can be attached to the pneumatic chamber.

3.3. General guidelines of the vacuum-driven micropumping

The design of vacuum-driven microfluidic devices depends on two parameters; (1) one is the volume ratio (α) between the whole PDMS device (or the PDMS membrane/wall) and the embedded microfluidic channels/chambers and (2) the other is the diffusion distance (l or w) from the embedded microfluidic channels/chambers to the outer surface of the PDMS device and/or the other side of the membrane.

In general, solubility-based devices require a relatively large amount of the volume ratio ($\alpha >> 1$), in order to imbibe the whole trapped air into the pre-vacuumed PDMS slab. However, permeability-based devices need to consist of about the same or less amount of the volume ratio ($\alpha \leq 1$), in order to allow fast air penetration through the PDMS membrane/wall. The volume of the embedded microfluidic channels/chambers should be about the same as that of the sample, to avoid any dead-volume for both types. Therefore, the solubility-based devices need to be thick enough to hold the vacuum inside the PDMS slab for a while, and the permeability-based devices require a thin PDMS membrane in order to permit instant steady-state air flux through the membrane.

To design proper vacuum-driven microfluidic devices utilizing the gas solubility or permeability of PDMS, first we need to calculate the time required for air diffusion over a given distance, as defined in **Eqn. (4).** This value is critical to estimate the degassing time and/or the working time of the device. The diffusion time increases with the square of diffusion distance. The diffusion time is inversely proportional to the diffusion coefficient. Assuming the diffusion coefficient is constant ($D \approx D_0 = D_{N2} = D_{O2} = 34\times10^{-6}$ cm^2/s), the

characteristic diffusion time constant (τ) is dependent on the thickness of the PDMS slab (l) or membrane (w).

For instance, a solubility-based PDMS device, with l = 2 mm and D_0 = 34×10^6 cm^2/s, has a characteristic time constant of τ = 7.9 min, indicating that the diffusion activity decays by a factor of 0.5 for ~5.5 min (see **Eqn. (4)**). Therefore, the working or operation time of the device is at most about 8 min. If you double the thickness of the PDMS slab with l = 4 mm, the characteristic time constant will be τ = 30 min, which means the power-free pumping ability will be kept much longer. However, if the characteristic time constant is too short, its power-free pumping ability will rapidly decay. In this case, multiple degassing may be needed to completely remove the air bubble and fill the dead-end microfluidic channels/chambers. An effective way to increase the working time is to coat the outer surface of the PDMS with a hermetic layer except the bottom of the device where contains the microfluidic channels, subsequently put the degassed PDMS slab on a glass slide to cover the bottom.

Characteristic time constants of a permeability-based PDMS device, with a thin PDMS wall thickness of w = 200 µm and a thick PDMS slab layer of l = 10 mm, are τ_w = 5 sec and τ_l = 3.3 hours, respectively. Once an external vacuum source is applied to a pneumatic pressure chamber, air diffusion from the dead-end channel to the pneumatic chamber through the thin PDMS wall or membrane will be stabilized within several seconds. As the gas permeation flux through the thin PDMS wall is more dominant than that through the thick PDMS slab from the outer surface (i.e., $w << l$), the order of generated vacuum level can be maintained in the pneumatic chamber for a long period of time (> ~1 hour). Increasing the surface area where the diffusion of the trapped air occurs and reducing the thickness of the PDMS wall or membrane will increase the flow rate (see **Eqn. (8)**).

As you can see from **Eqn. (7)** and **Eqn. (8),** the flow rate depends on k, an empirical factor related to the viscous effect of the pumped-in liquid, the flow hindrance effect of surface tension, and the geometry of the channel. The factor is inversely proportional to the hydraulic resistance of the microfluidic channel; therefore the volumetric flow rate can be faster with low-viscosity fluids, short channel lengths, large cross-sectional areas of the channel, and less hydrophobic surfaces. Note here that once the geometry of the PDMS microfluidic channel and the type of liquid are fixed, its hydraulic resistance (or the empirical factor k) can be considered to be constant. Although its hydraulic resistance will increase with time due to the traveling meniscus of the pumped-in liquids, it can be assumed constant; the effect of the pressure drop across the liquid and the meniscus will be negligible due to (1) the more dominant exponential decay effect for the solubility-based devices and (2) the much higher pressure difference across the PDMS membrane or wall for the permeability-based devices.

4. Applications of the vacuum-driven power-free microfluidics

Vacuum-driven power-free microfluidics is widely used for the air bubble removal and sample loading. Non-conventional applications cover mixing, viscosity measurement, blood separation and cell culture. This section focuses on real-life applications of using the vacuum-driven power-free microfluidics.

4.1. Air bubble removal and sample loading

The sample loading or priming without air traps is the most immediate problem encountered in the PDMS-based microfluidic experiments, because the surface of PDMS is naturally hydrophobic.[24] Several methods have been used to

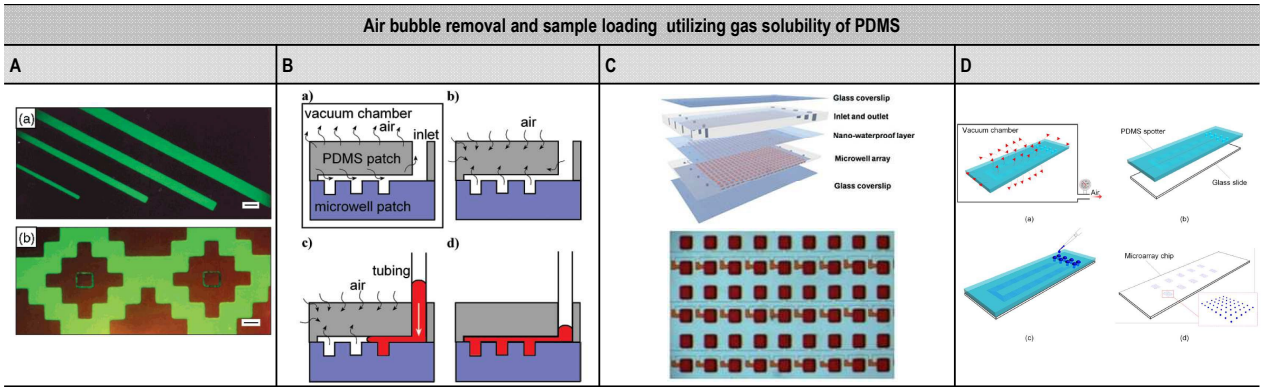

Fig. 4 Air bubble removal and sample loading utilizing gas solubility of PDMS. **[A]** (A-a) 35-125 µm ×10 µm PDMS terminated channels filled using a reduced-pressure chamber; (A-b) demonstration that only continuous fluidic networks are filled (the center 120 µm × 120 µm chamber is left unfilled); channel depth, 9 µm; scale bars indicates 120 µm. The fluorescence ring outlining the unfilled center squares is scattered light originating from the filled sections. **[B]** Schematic illustration of the method of dispensing liquid into an array of microwells through the degassed PDMS microchannel: (B-a) the degassing of the PDMS patch in a vacuum chamber, (B-b) the redissolving of air into PDMS from atmosphere, (B-c) the aspiration of the liquid into the microchannel and the microwells after a segment of tubing preloaded with the liquid was inserted into the inlet, and (B-d) the completion of the dispensing process when the liquid filled up the whole vacancy. **[C]** Upper: schematic drawing shows the design of the microfluidic chip for digital PCR. Bottom: All the microchambers were compartmentalized by oil. **[D]** Operating procedure of the PDMS spotter: (D-a) degassing of the PDMS spotter in a vacuum chamber, (D-b) reversible bonding of the spotter and glass slide under atmospheric conditions, (D-c) sample loading and dispensing after assembly, and (D-d) the removal of the spotter after biomolecules immobilization on the slide and the patterning of biomolecules remaining on the substrate. [A] from, [47] copyright American Chemical Society; [B] from, [48] copyright American Chemical Society; [C] from, [49] copyright Royal Society of Chemistry; [D] from, [50] copyright American Institute of Physics.

prime microfluidic devices without trapping of air bubbles. Flushing channels with isopropyl alcohol made trapped air bubbles to flow through more easily than water.[51] Another way to facilitate priming was to make the PDMS surface hydrophilic by exposing it to oxygen plasma.[52-54] However, the plasma-induced hydrophilicity is temporary and lost within a few hours. Therefore, in general, a capillary force or a pressure gradient by direct application of a vacuum at a reservoir outlet is not sufficient to completely fill complicated structures of the PDMS channels.[24]

Alternatively, vacuum-driven microfluidics utilizing the gas solubility or permeability of PDMS has been widely accepted in order to fill or prime liquid samples without any air bubble trapping in microfluidic channels.[47, 55, 56] This approach can easily solve such a problem, as shown in the following selected examples.

Utilizing gas solubility of PDMS

Fig. 4A shows complex microfluidic structures and arrays filled using a reduced-pressure chamber.[47] For the elimination of air bubbles, the sealed PDMS device bonded on a glass substrate was submerged into a filling solution of interest. The submerged device was then placed in a vacuum chamber to decrease the pressure which can allow air in the PDMS device to escape through inlets and outlets. Once the pressure was returned to atmospheric pressure, the filling process occurred in the PDMS device without any air bubbles trapped. This method was applicable to a variety of fluids, including phosphate buffered saline (PBS), Dulbecco's modified Eagle's medium (DMEM) and protein-supplemented (e.g., bovine serum) DMEM. The use of such fluids for priming is important when accurate concentrations are vital, such as in mammalian cell culture. It is proved that the proposed method is > 90% effective in removing the formation of bubbles in microfluidic channel networks.

Similarly, Zhou *et al*. developed a simple method to dispense a nanoliter volume of sample into microwell arrays by using degassed PDMS microchnnels as shown in **Fig. 4B**.[48] The degassed PDMS patch could act as an internal vacuum pumping source. The degassed PDMS patch could reversibly be bound onto a microwell patch. After a sample solution was aspirated into the microwell arrays through the PDMS channel, the PDMS microchannels were removed, resulting in arrays of droplets trapped in the microwells. Based on the proposed method, multiplex reactions were conducted for protein crystallization. In order to allow a long-term incubation, the microwells were fabricated on a glass, which enabled over two months of incubation. This method didn't require any sophisticated controlling systems, manufacturing and maintenance. In addition, different viscosity, surface tension, or clogs which may occur in dispensing technology cannot affect the filling procedure in the microwell arrays. The PDMS-based pumping technique provides a low-cost and simple platform for dispensing a nanoliter volume of liquid without air bubble formation inside. Based on the same principle, Zhu *et al*. proposed an integrated on-chip valve-free and power-free microfluidic digital polymerase-chain-reaction (PCR) device for single DNA molecule detection (**Fig. 4C**).[49, 57]

For patterning of microarrays, a spotter system was developed by Tang *et al*. who reported microchannels combined with a PDMS membrane containing thru-holes to spot biomolecules of interest on the glass microarray.[50] The spotter system consisted of reservoirs, microchannels, and arrays of thru-holes as shown in **Fig. 4D**. In order to deliver the protein sample on desired spots, the spotter system made by PDMS was degassed at 10 kPa for 2 hours in a vacuum chamber. The degassed PDMS spotter was assembled on a glass slide. Once the protein sample was filled and immobilized on the slide, the spotter system was removed, resulting in the patterning of biomolecules remaining on the substrate. The system provided a coefficient of variation of 2.63% in 48 spots. The conventional methods such as contact printing, in situ synthesis, and non-contact inkjet printing have limitations in optimization of critical parameters, including the viscosity and surface tension of sample, surface energy of nozzles. However, the proposed spotter system overcomes the limitations in that it offers low-cost in production, no external power source for pumping, and easy operation. In addition, the system is not sensitive to the specific fluid properties, which can enable reliable and uniform microarray patterns.

Utilizing gas permeability of PDMS

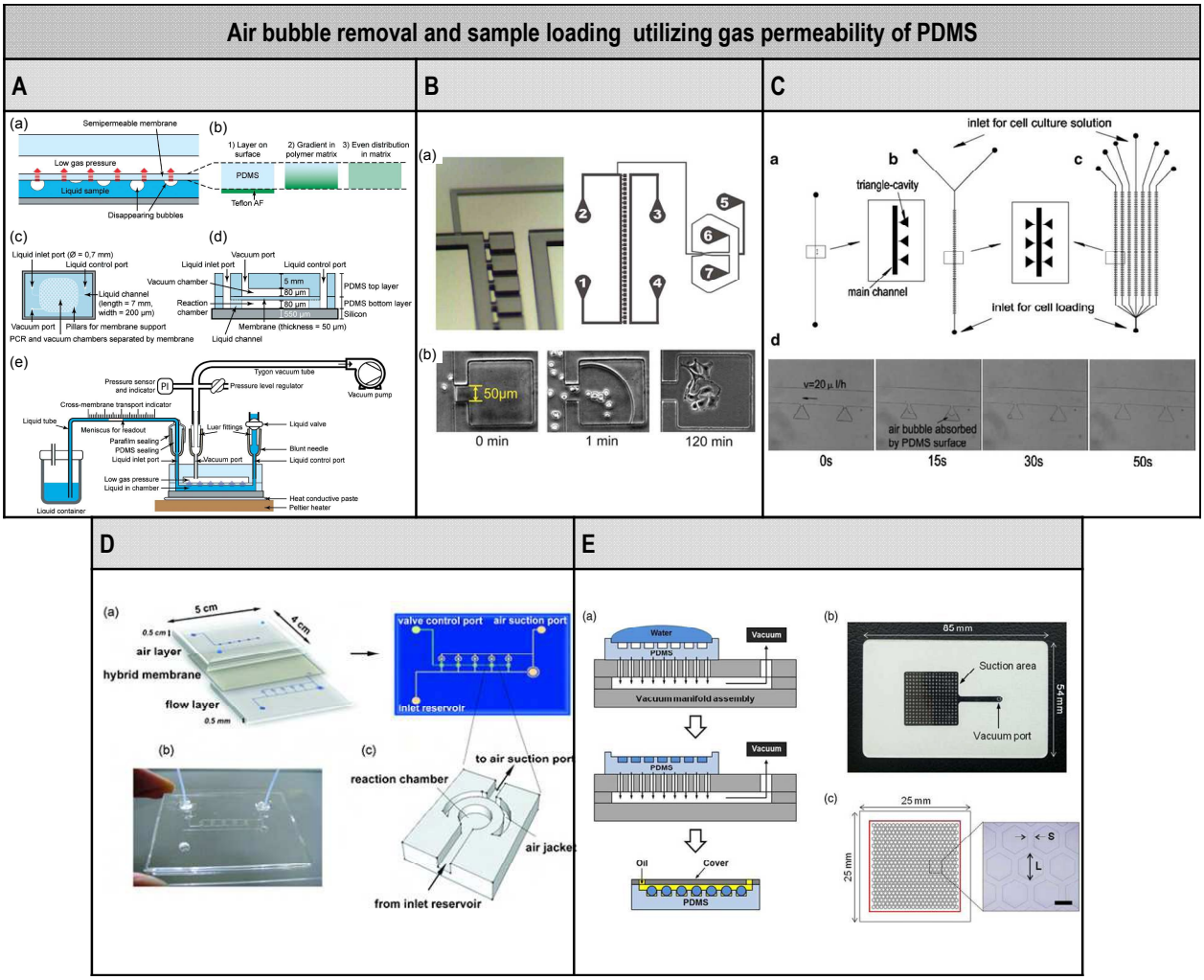

Fig. 5 Air bubble removal and sample loading utilizing gas permeability of PDMS. **[A]** (A-a) Debubbling principle, showing bubbles disappearing from a liquid-filled reaction chamber into a vacuum chamber. (A-b) Deposition of Teflon leads to three possible variants of Teflon distribution in PDMS. (A-c) Schematic top view and (A-d) cross-sectional side view showing dimensions of the microfluidic structure manufactured for permeability experiments. (A-e) Setup used for measurements of water loss through the semipermeable membrane. **[B]** Device design and vacuum loading of cells. (B-a) Each of the 33cuboid culture chambers is connected via a narrow opening to a main perfusion channel that runs between ports 1 and 2. A separate air channel between ports 3 and 4 allows the application of a temporary vacuum at the PDMS interface to draw fluid from the main perfusion channel into the culture chambers. Ports 5–7 comprise the DAW dynamic stimulation generator. (B-b) Upon application of a vacuum in the air channel at time zero, fluid containing cells is rapidly drawn into the culture chambers and fills the traps within 2 min, at which point the vacuum is turned off. HeLa cells attach and begin to spread out within 1–2 h after loading during continuous perfusion culture. **[C]** Masks for PDMS microfluidic device fabrication. (C-a) Three micro-triangle-cavities at one side of the main channel. (C-b) One single channel for cell culture (100 microcavities). (C-c) Seven parallel channels for different cell culture environments. (C-d) The microphotographs of air absorption in triangle cavities after water injection into the main channel. **[D]** The multi-chamber PCR chip platform. (D-a) On the left side, the structure of PCR chip with three layers: the air layer on the top, the thin Parylene-C – PDMS hybrid membrane for valve in the middle, and the flow layer at the bottom formed the PCR chip as shown on the right side. (D-b) The complete PDMS chip after fabrication. (D-c) The magnified reaction chamber with air jacket on the flow layer in chip. **[E]** (E-a) Schematics of the droplet-on-template procedure. The PDMS microwells are dead-end loaded with water by evacuating the trapped air in the wells through the PDMS template using the vacuum manifold assembly. Excess water is then removed by suction while the vacuum is maintained. Mineral oil is added through an inlet port of the acrylic cover bonded to the template, leading to the generation of a high density 2D DOT array. (E-b) A photograph of the vacuum manifold assembly (85 × 54 × 3 mm) is constructed by laminating three layers, including a white double-sided tape sandwiched between two acrylic sheets. The suction area (25 × 25 mm) is defined by patterning the double-sided tape. (E-c) A double-layered PDMS template with a square region (highlighted in red, 21 × 21 mm) in the upper layer and a honeycomb microwell array in the lower layer. The length and spacing of the microwells are denoted by L and S, respectively. Scale bar: 500 µm. [A] from, [58] copyright Royal Society of Chemistry; [B] from, [59] copyright Royal Society of Chemistry; [C] from, [60] copyright John Wiley and Sons; [D] from, [61] copyright Elsevier; [E] from, [62] copyright Institute of Physics.

Karlsson *et al.* developed an approach to remove air bubbles for microfluidic applications as shown in **Fig. 5A**.[58] The air bubbles trapped in a microfluidic PCR device were extracted from a reaction chamber to a vacuum chamber via a Teflon-coated PDMS membrane. The semipermeable membrane provided two functions; one was permeability of PDMS for air bubble extraction and the other was barrier property of Teflon to avoid water loss. With the coating of Teflon, the reduction in water or vapour loss was achieved whereas the air permeability was not significantly reduced. Based on this approach, they successfully demonstrated multiplex DNA amplification using PCR avoiding air bubbles. The water loss

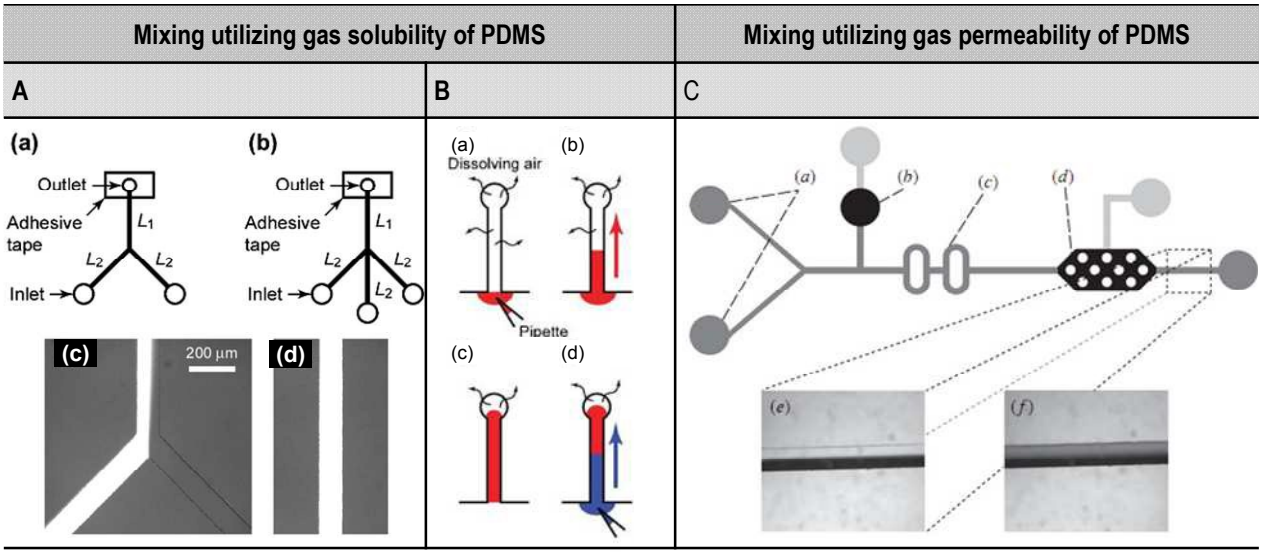

Fig. 6 Mixing utilizing gas solubility and permeability of PDMS. **[A]** Channel layouts of the PDMS microfluidic devices. (A-a) Two-inlet layout; (A-b) three-inlet layout. The following dimensions are common to both of these layouts. Channel cross-section: 100 mm (width) x 25 mm (height); channel lengths: 9.5 mm (L1) and 9.0 mm (L2); reservoir diameters: 2.0 mm (inlets) and 1.0 mm (outlet). (A-c) Image at the confluence. (A-d) Image at a downstream position. **[B]** Schematic representation of the first two steps in the power-free sequential injection. (B-a) Dispensing of the first aliquot. (B-b) Power-free pumping. (B-c) Retention of the solution by capillary force at the inlet. (B-d) Restart of the pumping by the second dispensing. **[C]** Bubble enhanced mixing apparatus schematic. (C-a) Fluid injection ports. A dyed water solution is pumped into one side of the channel and clear water into the other. (C-b) Bubble injection device. Applied pressure forces air through a membrane and into the fluid channel. (C-c) Mixing section. Bubbles enter the branched channels and force the fluid to fold over and cross streamlines to enhance mixing. (C-d) Bubble trap. Bubbles are trapped and removed in this section. (C-e) Photograph of fluid channel after the bubble trap with no bubble injection. The clear and dyed fluids are clearly discernible. (C-f) Photograph of fluid channel after the bubble trap with bubble injection. The clear and dyed fluids are markedly better mixed indicating the increased mixing efficiency from bubble inclusion. [A] from,[19] copyright Royal Society of Chemistry; [B] from, [27] copyright Royal Society of Chemistry; [C] from, [46] copyright Institute of Physics.

can be worsened at high temperature,[63-65] which can lead to failure in on-chip PCR. Permeability for water vapour is even 1–2 orders in magnitude higher than that for oxygen.[64]

Similarly, through a 2-dimensional design with all the channels in the same layer, Hasty *et al.* presented a trapping design to load a high density of cells into culture chambers that were isolated from flow sheering effect (**Fig. 5B**).[59] Qi *et al.* loaded cells into triangle-shape cavities within 1 min (**Fig. 5C**) [60] and Takamura *et al.* demonstrated air bubble free filling of a multi-chamber PCR chip based on the same principle (**Fig. 5D**).[61] In addition, through the help of a customized holder, Song *et al.* presented a method for generating a high-density droplet array within honeycomb micro-wells through utilizing the gas permeability of PDMS (**Fig. 5E**).[62]

4.2. Mixing

Another unique feature of utilizing the gas solubility or permeability of PDMS is that the sample loading will start only after all the inlets are covered by sample liquids. Therefore, as demonstrated by **Fig. 6A**,[19] two or more different types of liquids can flow at the same or different flow rates depending on the fluidic resistance ratios between the channels.[66] These liquids could be mixed in the dead-end main channel for a variety of reactions, such as immunoassay testing,[45] DNA[19, 28, 67] or RNA[30] analysis, or mercury detection.[29]

Moreover, even for a single inlet dead-end microfluidic channel, sequential injection of two different liquids is demonstrated for heterogeneous immunoassay, as shown in **Fig. 6B**.[27] Combined with a capillary valve effect, the meniscus of the first liquid will be held at the inlet even though the dead-end microfluidic channel is not fully filled. Then the second liquid can be added at the inlet and follow the previously filled liquid towards the end of the channel. The power-free sequential injection with the sample consumption of 1 μL enabled sandwich immunoassay for rabbit immunoglobulin G (rIgG) and human C-reactive protein (CRP) with a detection limit of 0.21 nM and 0.42 nM, respectively.

The mixing can be even more effective by employing the micropumping utilizing the gas permeability of PDMS. Because this method could control the trapped air inside the microfluidic channels in a bidirectional fashion, air bubbles could be ejected into the flow channels by high pressure firstly to enhance the mixing of liquids. Then the air bubbles could be removed by applying low pressure at the air bubble trapping site (**Fig. 6C**).[46]

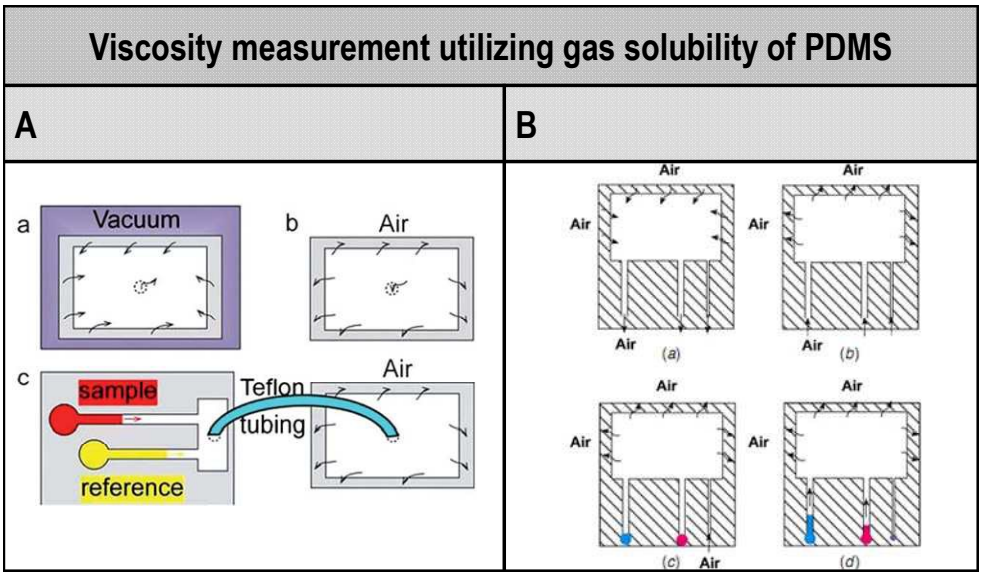

Fig. 7 Viscosity measurement utilizing gas solubility of PDMS. **[A]** A schematic illustration of the measurement process. (A-a) The PDMS pump was degassed in a vacuum desiccator for 15 min and the air in PDMS was depleted. (A-b) The degassed PDMS pump was brought back into the atmosphere, and air went through the inlet to the internal chamber and then diffused into PDMS. (A-c) The PDMS pump was connected with PDMS viscometer by Teflon tubing. Sample and reference started to flow in the channel. **[B]** Schematic illustration of the method of dispensing liquid into an array of microwells through the degassed PDMS microchannel: (B-a) the degassing of the PDMS patch in a vacuum chamber, (B-b) the redissolving of air into PDMS from atmosphere, (B-c) the aspiration of the liquid into the microchannel and the microwells after a segment of tubing preloaded with the liquid was inserted into the inlet, and (B-d) the completion of the dispensing process when the liquid filled up the whole vacancy. [A] from, [68] copyright Royal Society of Chemistry; [B] from, [69] copyright Institute of Physics.

4.3. Viscosity measurement

Through employing a degassed PDMS chamber as a vacuum pump, a microfluidic device for measuring the viscosity of Newtonian fluids was proposed by Zheng *et al* (**Fig. 7A**).[68] By monitoring the flow rates of both sample and reference fluids in the dead-end microfluidic channels, the viscosity of the sample liquid (i.e., the activity of endo-β-1,4-glucanases on hydrolyzing sodium carboxymethylcellulose) was measured at different reaction times. In a similar way, a degassed PDMS viscometer was proposed for microliter Newtonian fluids, including aqueous solutions, non-PDMS-swelling organic solvents, fluorinated oil and blood plasma (**Fig. 7B**).[69]

4.4. Blood separation

Sample preparation, particularly for blood plasma separation from whole blood, is a key function for POC microfluidic devices.[71] A lot of blood separation methods have been developed through employing microfluidic devices.[72-76] Among them, sedimentation seems to be a very favourable way to separate haemolysis-free plasma from whole blood.[77-81] Because of the density difference between blood cells and plasma, blood cells tend to be deposited toward the gravity direction at stable or quasi-stable states. Because the flow rates are relatively low in the vacuum-driven power-free micropumping, it is very suitable for the sedimentation based blood separation.

Fig. 8A gives an example of blood separation based on the micropumping utilizing the gas solubility of PDMS.[43] By adding trenches in the microfluidic channels, Lee *et al.* proposed a device to extract blood plasma from a 5 µL droplet of whole blood. The device was also integrated with an ELISA assay for biotin detection. In this study, the image analysis showed 100% plasma purity and the biotin spiked blood samples were detected by fluorescent measurement in concentrations as low as 1.5 pM. However, due to the relatively large size of the trench (i.e., 2 mm in depth, 1 mm in diameter) and inconsistent flow, the yield of plasma from whole blood was not high (~1%).

To get a higher plasma separation yield, another blood separation method employing sedimentation based blood separation and permeation based micropumping was proposed by Xu *et al* (**Fig. 8B**).[70] In this study, manually operating syringes were employed as mobile vacuum sources, which were connected to pneumatic chambers. The separation chamber and pneumatic chambers were isolated by a thin PDMS wall. By pulling out the plunger of the syringes to 2 mL, a low vacuum was immediately formed in the small pneumatic chambers (~2 µL). Based on a rough estimation using an ideal gas equation: $p_1V_1 = nRT = p_2V_2$, the vacuum level inside the pneumatic chamber becomes 100 Pa from 100 kPa.

In the design, to facilitate the blood filling and separation process, a triangular separation chamber was embedded with phaseguide structures. By controlling the overlap surface area and the thickness of the PDMS wall between the separation chamber and the vacuumed pneumatic chamber, a constant and controllable flow rate was achieved. Combined with the modified phaseguide structures, around 0.38 µL of plasma was separated from 2 µL of whole blood. Furthermore, air bubbles diffused into a ring channel by a positive pressure gradient enabled the retrieval of the separated plasma from the dead-end chamber on demand.

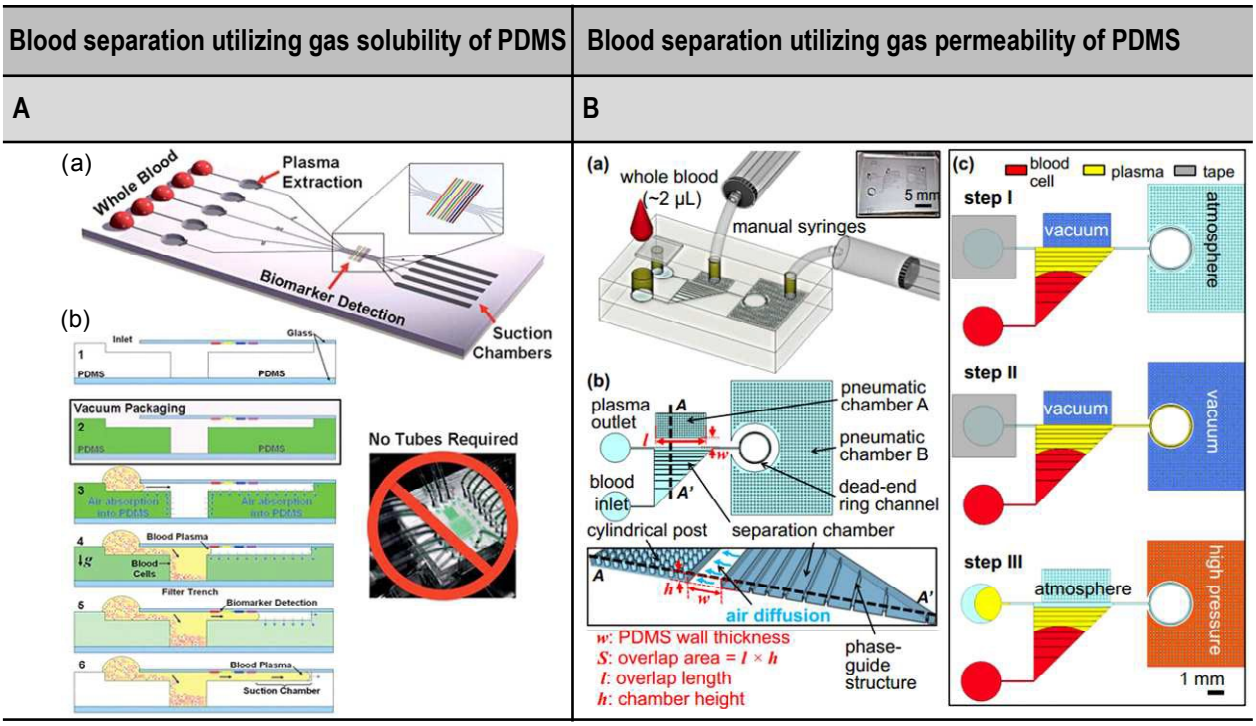

Fig. 8 Blood separation utilizing gas solubility and permeability of PDMS. **[A]** Self-priming, self-contained, tether-free SIMBAS (A-a) integrates (i) volume-metering (ii) plasma separation from whole-blood (iii) multiple biomarker detection and (iv) suction chambers for fluid propulsion. (A-b) Cross section of device operation. **[B]** Schematics of the proposed device. (B-a) Overview of the experimental setup with the proposed device. The top layer is a PDMS cover with an inlet, a tape-sealed outlet and is bonded irreversibly with a bottom fluidic layer. (B-b) Top view and cross-section view. The separation chamber is divided into ten segments with equal volume by nine phaseguides at the bottom. Cylindrical posts are used to prevent the collapsing of the pneumatic chamber when it is vacuumed by the manual syringes. w and S stand for the PDMS wall thickness and the overlap area between the pneumatic chamber A and the separation chamber, respectively. The overlap area (S), where the flux of air diffuses, is calculated by the overlap length (l) multiplied by the chamber height (h). Drawings are not to scale. (B-c) Experimental steps. [A] from, [43] copyright Royal Society of Chemistry; [B] from,[70] copyright American Institute of Physics.

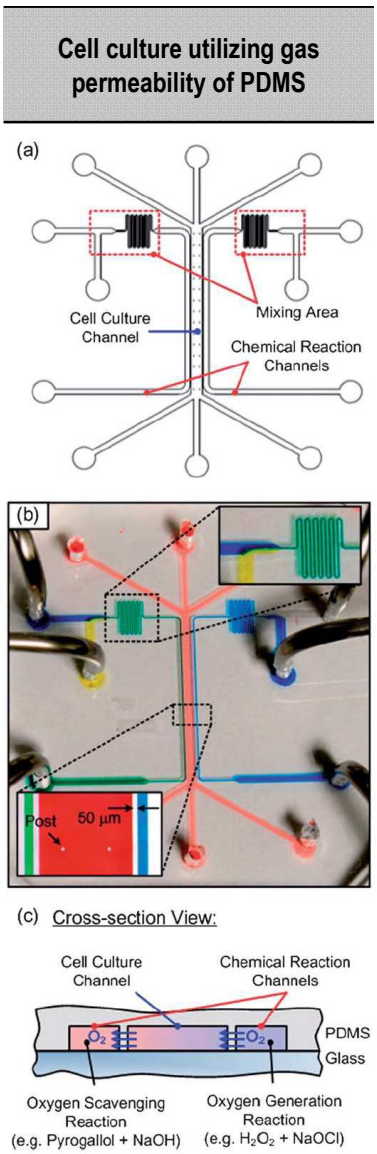

Fig. 9 Cell culture utilizing gas permeability of PDMS. (a) The schematic of the device with three sets of microfluidic channel patterns. (b) Photo of the fabricated device filled with food dyes. (c) The cross-sectional view showing the working principle of the device. [82] Copyright Royal Society of Chemistry.

4.5. Cell culture

The high gas permeability of PDMS is mostly beneficial to supply of oxygen, especially in microfluidic cell culture devices.[64, 83] The most straightforward approach for oxygen control in the devices is by diffusion from a pre-equilibrated liquid flowing through the device's control channels across a gas permeable PDMS membrane and into the cell culture region.[84] Another way is to flow gas directly though the control channels, eliminating the need for the pre-equilibration of liquid off-chip.[83, 85] A variety of oxygen control methods, such as discrete control,[86] spatial control,[87, 88] and temporal control,[87] has been demonstrated.

However, dehydration of culture media is a common disadvantage of flowing dry gas over the diffusion membrane in microfluidic cell culture systems. To solve this problem, Wood *et al*. added a hydration layer, which is an additional liquid (e.g., PBS buffer) filled channel between the gas layer and culture or sample layer.[89] This configuration could prevent dehydration of blood sample while allowing the transport of oxygen in a microfluidic device.

Oxygen can also be modulated by on-chip chemical reactions that either generate or scavenge oxygen. Chen *et al.* reported a microfluidic cell culture device generating oxygen gradients, caused by using a pair of chemical reactions, as shown in **Fig. 9**.[82] The device consisted of three single-layer channels; a middle cell culture channel was bordered on either side with a chemical reaction channel. An oxygen gradient was formed across the middle channel by an oxygen generating reaction (e.g., H_2O_2 + NaOCl) in one reaction channel and an oxygen scavenging reaction (e.g., pyrogallol + NaOH) in the other reaction channel. Based on the two chemical reactions, various oxygen gradients could be achieved in the middle channel for cell culture. For a proof of concept, carcinomic human alveolar basal epithelial (A549) cells were cultured in the proposed microfluidic device with a culture medium and an anti-cancer drug (Tirapazamine, TPZ) under different oxygen gradients.

5. Conclusions and outlook

5.1 Summary

The use of the micropumping based on the gas solubility or permeability of PDMS is a very powerful and straightforward tool for point-of-care microfluidic systems. The method usually requires very low energy consumption, or pre-stored energy, without external power or a moving part to generate a sufficient flow rate. Meanwhile, air bubble-free filling can be achieved no matter that how complicated of the channel design and the surface property of the channel is. Numerous applications for air bubble removal, sample loading, mixing, viscosity measurement, blood separation and cell cultures have been developed to investigate various chemical and biological questions in POC diagnostics.

5.2 Advanced aspects and outlook

In this section, we briefly overview selected advanced topics and the outlook in using the micropumping utilizing the gas solubility or permeability of PDMS: limitations, pumping rates, flow control, other materials, vacuum generation, and water vapour or solvent permeation effects.

Limitations. PDMS needs to be the material of the device to employ this pumping method. Moreover, for the micropumping utilizing the gas solubility of PDMS, its pumping power decreases fast after the pre-vacuumed PDMS devices are placed under atmosphere. Also the PDMS devices need to be pre-vacuumed for a sufficient time and be stored in an air-tight package before use. And once the device is filled with liquid, the micropumping will no longer work.

For the micropumping utilizing the gas permeability of PDMS, even though better flow control can be achieved by both surface area and thickness of the PDMS membrane or PDMS wall, the range of the flow rates is still limited to one order. In addition, if a PDMS membrane is employed, fabrication cost and time will increase (bonding and alignment are needed). And if a PDMS wall is employed, the density of microfluidic channels will decrease a lot as the surrounding pneumatic microchambers will take some space.

Pumping rates. Intrinsically, the flow rates by this pumping method are limited to ~nL/s due to the limited air diffusion and the hydrophobicity of the PDMS. As indicated in **Eqn. (7)** and **Eqn. (8)**, by increasing the total surface area allowing air to diffuse, the vacuum-driven power-free pumping will be greatly enhanced, such as using a comb-like pneumatic chamber.[20, 25] Whereas, if the channel surface is hydrophilic like glass, the flow rates can be increased 10 to 100 times as shown in **Fig. 3**.[46] Therefore, surface coating of the channel making the surface more hydrophilic may help increasing the pumping rates.

Flow control. Like the capillary driven microfluidics, structure-dependent passive valving combined with the vacuum-driven power-free microfluidics might be a good solution to control the flow (i.e., stop or delay). For example, a recent work showed that geometry-assisted meniscus priming by placing phaseguiding structures on the surface of channels could control priming and emptying in a step-wise manner between phaseguides.[90] Xu *et al.* demonstrated phaseguide-assisted vacuum-driven microfluidics, in order to enhance efficient priming of whole blood and its sedimentation-based plasma separation.[70] Also, they suggested a step-wise channel height, width or length variation could provide the ability of stopping, delaying, guiding or synchronized merging of flows in the vacuum-driven microfluidics. Because air bubbles can easily block the fluidic path in microfluidic channels,[91-94] a combination of the injection and removal of small air bubbles through the gas permeable PDMS[25, 70] may allow to design a smart in-line flow control system.

Materials. Theoretically, as long as the material has similar gas solubility and permeability to PDMS, the micropumping method should be able to work. Recently, Lee *et al*. reported a similar pumping method by utilizing the gas permeability of silicone tube and a hand-held syringe to control the sample flow for on-chip continuous-flow PCR.[95] Yuen *et al*. suggested controllable porosities of PDMS by a mixture of PDMS pre-polymer and sugar particles for cell culture applications where gas perfusion can improve cell survival and functions.[96, 97] Cha and Kim proposed a portable pressure pump using such a porous PDMS sponge.[98]

In general, polymers with high gas permeability are generally less selective to gas species,[99] and similarly PDMS is also a non-selective polymer, allowing most of the gases to effectively permeate through the material (**Table 1**). In order to improve selectivity within polymers, researchers have been considering the use of fillers for creating unique composites.[100] For example, adding carbon-based fillers, such as carbon nanotube (CNTs), carbon black (CB) and graphene, can offer PDMS composites the capability of tuning properties, such as conductivity, strength and gas selectivity.[101] By incorporating the carbon-based fillers within PDMS in the vacuum-driven power-free microfluidics, one may come up with a new class of gas sensing applications.

Vacuum generation. In this vacuum-driven power-free microfluidics, low vacuum is enough to operate with the pressure one to two orders of magnitude lower than atmospheric pressure (i.e., 0.1 to 0.01 atm). Such a vacuum level can be easily achievable by using normal vacuum desiccators[19] or even hand-held syringes.[25, 33, 70, 102] For the on-site application, the testing PDMS chip can be pre-packaged in a vacuum sealer that is commonly used for medical devices, requiring an immediate use after unpacking.[43, 103] For the permeation based micropumping application, adequate vacuum level can be on-demand generated by a hand-held syringe[25] or a 3D printed suction cup.[31] An interesting concept of using vacuum capillary pneumatic actuation was suggested by Weng *et al*.[104] They encapsulated a vacuum glass capillary within a laminated pouch and broke the capillary by finger pressure in order to generate the vacuum energy in the POC fluidic system. Hong and Cheng employed pre-programmable polymer transformers (i.e., thermally actuated shape memory polymer (SMP) materials) as on-chip microfluidic vacuum generators.[105]

Permeation of water vapour or solvent. Until now, water permeability into PDMS has been considered negligible for most microfluidic applications due to $D_{Water} = 8.5\times10^{-6}$ cm^2/s << $D_{N2} = D_{O2} = 34\times10^{-6}$ cm^2/s.[63] Worse yet, it is well known that high permeation to organic solvents is one of the main drawbacks of using PDMS.[106] Randall and Doyle showed that small but finite permeability could generate a significant passive flow in thin channels, as device size decreases because the surface area to volume ratio increases.[63] In droplet-based microfluidics, the droplet size and its volume are so small that the evaporation of water could form a serious issue for long-term assay or incubation.[107] To prevent the shrinkage of droplets, resulting from such water or solvent permeation effects, PDMS devices were placed in humidified chamber (saturated with H_2O) or under water environment,[108, 109] or the surface of PDMS devices were coated with non-permeable materials (i.e., Teflon Amorphous Fluoropolymer,[58] Parylene[110]). Rather than avoiding the evaporation effects, harnessing such effects could lead to new applications, such as protein crystallization in aqueous droplets,[109] bead stacking,[63] chemical concentration, and passive pumping.[63]

We expect that microfluidics and LOC communities will be able to harness vacuum energy to develop unique microfluidic applications to advance many biological, chemical, pharmaceutical, and other scientific and technical challenges.

Acknowledgements

This work was partially supported by the National Science Foundation grants (Grant Nos. CBET-1403086, CBET-1337860, ECCS-1002255, DBI-0959989 and ECCS-0736501) and a grant from Qualcomm Incorporated.

Notes and references

1. L. Gervais, N. De Rooij and E. Delamarche, Microfluidic Chips for Point-of-Care Immunodiagnostics, *Advanced materials*, 2011, 23, H151-H176.
2. R. Sista, Z. Hua, P. Thwar, A. Sudarsan, V. Srinivasan, A. Eckhardt, M. Pollack and V. Pamula, Development of a digital microfluidic platform for point of care testing, *Lab Chip*, 2008, 8, 2091-2104.
3. L. Gervais and E. Delamarche, Toward one-step point-of-care immunodiagnostics using capillary-driven microfluidics and PDMS substrates, *Lab Chip*, 2009, 9, 3330-3337.
4. S. K. Sia and L. J. Kricka, Microfluidics and point-of-care testing, *Lab Chip*, 2008, 8, 1982-1983.
5. F. B. Myers and L. P. Lee, Innovations in optical microfluidic technologies for point-of-care diagnostics, *Lab Chip*, 2008, 8, 2015-2031.
6. S. Moon, H. O. Keles, A. Ozcan, A. Khademhosseini, E. Hæggstrom, D. Kuritzkes and U. Demirci, Integrating microfluidics and lensless imaging for point-of-care testing, *Biosensors Bioelectronics*, 2009, 24, 3208-3214.
7. D. Laser and J. Santiago, A review of micropumps, *Journal of micromechanics and microengineering*, 2004, 14, R35.
8. B. D. Iverson and S. V. Garimella, Recent advances in microscale pumping technologies: a review and evaluation, *Microfluidics Nanofluidics*, 2008, 5, 145-174.
9. P. Gravesen, J. Branebjerg and O. S. Jensen, Microfluidics-a review, *Journal of Micromechanics and Microengineering*, 1993, 3, 168.
10. M. De Volder and D. Reynaerts, Pneumatic and hydraulic microactuators: a review, *Journal of Micromechanics and microengineering*, 2010, 20, 043001.
11. K. W. Oh and C. H. Ahn, A review of microvalves, *Journal of Micromechanics and Microengineering*, 2006, 16, R13-R39.
12. N. S. Lynn and D. S. Dandy, Passive microfluidic pumping using coupled capillary/evaporation effects, *Lab Chip*, 2009, 9, 3422-3429.
13. G. M. Walker and D. J. Beebe, A passive pumping method for microfluidic devices, *Lab Chip*, 2002, 2, 131-134.
14. M. Zimmermann, S. Bentley, H. Schmid, P. Hunziker and E. Delamarche, Continuous flow in open microfluidics using controlled evaporation, *Lab Chip*, 2005, 5, 1355-1359.
15. N. Goedecke, J. Eijkel and A. Manz, Evaporation driven pumping for chromatography application, *Lab Chip*, 2002, 2, 219-223.
16. W. Li, T. Chen, Z. Chen, P. Fei, Z. Yu, Y. Pang and Y. Huang, Squeeze-chip: a finger-controlled microfluidic flow network device and its application to biochemical assays, *Lab Chip*, 2012, 12, 1587-1590.
17. E. Berthier and D. J. Beebe, Flow rate analysis of a surface tension driven passive micropump, *Lab Chip*, 2007, 7, 1475-1478.
18. J. S. Rossier, S. Baranek, P. Morier, C. Vollet, F. Vulliet, Y. De Chastonay and F. Reymond, GRAVI: robotized microfluidics for fast and automated immunoassays in low volume, *Journal of the Association for Laboratory Automation*, 2008, 13, 322-329.
19. K. Hosokawa, K. Sato, N. Ichikawa and M. Maeda, Power-free poly (dimethylsiloxane) microfluidic devices for gold nanoparticle-based DNA analysis, *Lab Chip*, 2004, 4, 181-185.
20. D. Y. Liang, A. M. Tentori, I. K. Dimov and L. P. Lee, Systematic characterization of degas-driven flow for poly (dimethylsiloxane) microfluidic devices, *Biomicrofluidics*, 2011, 5, 024108.
21. M. A. Eddings and B. K. Gale, A PDMS-based gas permeation pump for on-chip fluid handling in microfluidic devices, *Journal of Micromechanics and Microengineering*, 2006, 16, 2396.
22. H. Wu, A. Wheeler and R. N. Zare, Chemical cytometry on a picoliter-scale integrated microfluidic chip, *Proc Natl Acad Sci*, 2004, 101, 12809-12813.
23. W. L. Ong, K. C. Tang, A. Agarwal, R. Nagarajan, L. W. Luo and L. Yobas, Microfluidic integration of substantially round glass capillaries for lateral patch clamping on chip, *Lab Chip*, 2007, 7, 1357-1366.
24. J. H. Kang, Y. C. Kim and J.-K. Park, Analysis of pressure-driven air bubble elimination in a microfluidic device, *Lab Chip*, 2008, 8, 176-178.
25. L. Xu, H. Lee and K. W. Oh, Syringe-assisted point-of-care micropumping utilizing the gas permeability of polydimethylsiloxane, *Microfluidics Nanofluidics*, 2014, 17, 745-750.
26. T. Merkel, V. Bondar, K. Nagai, B. Freeman and I. Pinnau, Gas sorption, diffusion, and permeation in poly (dimethylsiloxane), *Journal of Polymer Science Part B: Polymer Physics*, 2000, 38, 415-434.
27. K. Hosokawa, M. Omata, K. Sato and M. Maeda, Power-free sequential injection for microchip immunoassay toward point-of-care testing, *Lab Chip*, 2006, 6, 236-241.
28. Y. Sato, K. Sato, K. Hosokawa and M. Maeda, Surface plasmon resonance imaging on a microchip for detection of DNA-modified gold nanoparticles deposited onto the surface in a non-cross-linking configuration, *Anal Biochem*, 2006, 355, 125-131.
29. S. He, D. Li, C. Zhu, S. Song, L. Wang, Y. Long and C. Fan, Design of a gold nanoprobe for rapid and portable mercury detection with the naked eye, *Chem. Commun.*, 2008, 4885-4887.
30. H. Arata, K. Hosokawa and M. Maeda, Rapid Sub-attomole MicroRNA Detection on a Portable Microfluidic Chip, *Analytical Sciences*, 2014, 30, 129-135.
31. S. Begolo, D. V. Zhukov, D. A. Selck, L. Li and R. F. Ismagilov, The pumping lid: investigating multi-material 3D printing for equipment-free, programmable generation of positive and negative pressures for microfluidic applications, *Lab Chip*, 2014, 14, 4616-4628.
32. C. G. Li, M. Dangol, C. Y. Lee, M. Jang and H. Jung, A self-powered one-touch blood extraction system: a novel polymer-capped hollow microneedle integrated with a pre-vacuum actuator, *Lab Chip*, 2015, 15, 382-390.
33. A. R. Abate and D. A. Weitz, Syringe-vacuum microfluidics: A portable technique to create monodisperse emulsions, *Biomicrofluidics*, 2011, 5, 14107.
34. M. A. Unger, H. P. Chou, T. Thorsen, A. Scherer and S. R. Quake, Monolithic microfabricated valves and pumps by multilayer soft lithography, *Science*, 2000, 288, 113-116.
35. P. N. Duncan, T. V. Nguyen and E. E. Hui, Pneumatic oscillator circuits for timing and control of integrated microfluidics, *Proc Natl Acad Sci*, 2013, 110, 18104-18109.

36. Y. Xia and G. M. Whitesides, Soft lithography, *Annual Review of Materials Science*, 1998, 28, 153-184.
37. G. M. Whitesides, E. Ostuni, S. Takayama, X. Jiang and D. E. Ingber, Soft lithography in biology and biochemistry, *Annual Review of Biomedical Engineering*, 2001, 3, 335-373.
38. B.-H. Jo, L. M. Van Lerberghe, K. M. Motsegood and D. J. Beebe, Three-dimensional micro-channel fabrication in polydimethylsiloxane (PDMS) elastomer, *Journal of Microelectromechanical Systems*, 2000, 9, 76-81.
39. J. R. Anderson, D. T. Chiu, R. J. Jackman, O. Cherniavskaya, J. C. McDonald, H. Wu, S. H. Whitesides and G. M. Whitesides, Fabrication of topologically complex three-dimensional microfluidic systems in PDMS by rapid prototyping, *Anal Chem*, 2000, 72, 3158-3164.
40. T. Fujii, PDMS-based microfluidic devices for biomedical applications, *Microelectronic Engineering*, 2002, 61, 907-914.
41. H. Czichos, T. Saito and L. R. Smith, *Springer handbook of materials measurement methods*, Springer, Germany, 2006.
42. K. Ghosal and B. D. Freeman, Gas separation using polymer membranes: an overview, *Polymers for Advanced Technologies*, 1994, 5, 673-697.
43. I. K. Dimov, L. Basabe-Desmonts, J. L. Garcia-Cordero, B. M. Ross, A. J. Ricco and L. P. Lee, Stand-alone self-powered integrated microfluidic blood analysis system (SIMBAS), *Lab Chip*, 2011, 11, 845-850.
44. G. Li, Y. Luo, Q. Chen, L. Liao and J. Zhao, A "place n play" modular pump for portable microfluidic applications, *Biomicrofluidics*, 2012, 6, 014118.
45. K. Hosokawa, M. Omata and M. Maeda, Immunoassay on a power-free microchip with laminar flow-assisted dendritic amplification, *Anal Chem*, 2007, 79, 6000-6004.
46. M. Johnson, G. Liddiard, M. Eddings and B. Gale, Bubble inclusion and removal using PDMS membrane-based gas permeation for applications in pumping, valving and mixing in microfluidic devices, *Journal of Micromechanics and Microengineering*, 2009, 19, 095011.
47. J. Monahan, A. A. Gewirth and R. G. Nuzzo, A method for filling complex polymeric microfluidic devices and arrays, *Anal Chem*, 2001, 73, 3193-3197.
48. X. Zhou, L. Lau, W. W. L. Lam, S. W. N. Au and B. Zheng, Nanoliter dispensing method by degassed poly (dimethylsiloxane) microchannels and its application in protein crystallization, *Anal Chem*, 2007, 79, 4924-4930.
49. Q. Zhu, L. Qiu, B. Yu, Y. Xu, Y. Gao, T. Pan, Q. Tian, Q. Song, W. Jin and Q. Jin, Digital PCR on an integrated self-priming compartmentalization chip, *Lab Chip*, 2014, 14, 1176-1185.
50. T. Tang, G. Li, C. Jia, K. Gao and J. Zhao, An equipment-free polydimethylsiloxane microfluidic spotter for fabrication of microarrays, *Biomicrofluidics*, 2014, 8, 026501.
51. K. E. Herold and A. Rasooly, *Lab on a chip technology*, Caister Academic Press, Norfolk, UK, 2009.
52. M. Fuerstman and K. Samuel, Mixing with bubbles: a practical technology for use with portable microfluidic devices, *Lab Chip*, 2006, 6, 207-212.
53. S. K. Sia and G. M. Whitesides, Microfluidic devices fabricated in poly (dimethylsiloxane) for biological studies, *Electrophoresis*, 2003, 24, 3563-3576.
54. H.-B. Liu, H.-Q. Gong, N. Ramalingam, Y. Jiang, C.-C. Dai and K. M. Hui, Micro air bubble formation and its control during polymerase chain reaction (PCR) in polydimethylsiloxane (PDMS) microreactors, *Journal of Micromechanics and Microengineering*, 2007, 17, 2055.
55. F. Burgoyne, in *Chips and Tips*, Royal Siciety of Chemistry, Lab Chip, 2006, vol. 2015.
56. J. T. Nevill, A. Mo, B. J. Cord, T. D. Palmer, M. M. Poo, L. P. Lee and S. C. Heilshorn, Vacuum soft lithography to direct neuronal polarization, *Soft Matter*, 2011, 7, 343-347.
57. Q. Zhu, Y. Gao, B. Yu, H. Ren, L. Qiu, S. Han, W. Jin, Q. Jin and Y. Mu, Self-priming compartmentalization digital LAMP for point-of-care, *Lab Chip*, 2012, 12, 4755-4763.
58. J. M. Karlsson, M. Gazin, S. Laakso, T. Haraldsson, S. Malhotra-Kumar, M. Mäki, H. Goossens and W. van der Wijngaart, Active liquid degassing in microfluidic systems, *Lab Chip*, 2013, 13, 4366-4373.
59. M. Kolnik, L. S. Tsimring and J. Hasty, Vacuum-assisted cell loading enables shear-free mammalian microfluidic culture, *Lab Chip*, 2012, 12, 4732-4737.
60. C. Luo, X. Zhu, T. Yu, X. Luo, Q. Ouyang, H. Ji and Y. Chen, A fast cell loading and high-throughput microfluidic system for long-term cell culture in zero-flow environments, *Biotechnology Bioengineering*, 2008, 101, 190-195.
61. N. B. Trung, M. Saito, H. Takabayashi, P. H. Viet, E. Tamiya and Y. Takamura, Multi-chamber PCR chip with simple liquid introduction utilizing the gas permeability of polydimethylsiloxane, *Sensors and Actuators B: Chemical*, 2010, 149, 284-290.
62. J. Kim and S. Song, On-chip high density droplet-on-template (DOT) array, *Journal of Micromechanics and Microengineering*, 2015, 25, 017001.
63. G. C. Randall and P. S. Doyle, Permeation-driven flow in poly(dimethylsiloxane) microfluidic devices, *Proc Natl Acad Sci*, 2005, 102, 10813-10818.
64. J. de Jong, R. G. Lammertink and M. Wessling, Membranes and microfluidics: a review, *Lab Chip*, 2006, 6, 1125-1139.
65. K. W. Oh, C. Park, K. Namkoong, J. Kim, K. S. Ock, S. Kim, Y. A. Kim, Y. K. Cho and C. Ko, World-to-chip microfluidic interface with built-in valves for multichamber chip-based PCR assays, *Lab Chip*, 2005, 5, 845-850.
66. K. W. Oh, K. Lee, B. Ahn and E. P. Furlani, Design of pressure-driven microfluidic networks using electric circuit analogy, *Lab Chip*, 2012, 12, 515-545.
67. J. Li, Y. Huang, D. Wang, B. Song, Z. Li, S. Song, L. Wang, B. Jiang, X. Zhao, J. Yan, R. Liu, D. He and C. Fan, A power-free microfluidic chip for SNP genotyping using graphene oxide and a DNA intercalating dye, *Chem Commun (Camb)*, 2013, 49, 3125-3127.
68. X. Tang and B. Zheng, A PDMS viscometer for assaying endoglucanase activity, *Analyst*, 2011, 136, 1222-1226.
69. Z. Han, X. Tang and B. Zheng, A PDMS viscometer for microliter Newtonian fluid, *Journal of Micromechanics and Microengineering*, 2007, 17, 1828.
70. L. Xu, H. Lee, M. V. Brasil Pinheiro, P. Schneider, D. Jetta and K. W. Oh, Phaseguide-assisted blood separation microfluidic device for point-of-care applications, *Biomicrofluidics*, 2015, 9, 014106.

71. M. Kersaudy-Kerhoas and E. Sollier, Micro-scale blood plasma separation: from acoustophoresis to egg-beaters, *Lab Chip*, 2013, 13, 3323-3346.
72. M. Toner and D. Irimia, Blood-on-a-chip, *Annual Review of Biomedical Engineering*, 2005, 7, 77-103.
73. S. Yang, A. Ündar and J. D. Zahn, A microfluidic device for continuous, real time blood plasma separation, *Lab Chip*, 2006, 6, 871-880.
74. M. Kersaudy-Kerhoas, R. Dhariwal, M. P. Desmulliez and L. Jouvet, Hydrodynamic blood plasma separation in microfluidic channels, *Microfluidics Nanofluidics*, 2010, 8, 105-114.
75. S. Yang, A. Ündar and J. D. Zahn, Blood plasma separation in microfluidic channels using flow rate control, *Asaio Journal*, 2005, 51, 585-590.
76. X. Yang, O. Forouzan, T. P. Brown and S. S. Shevkoplyas, Integrated separation of blood plasma from whole blood for microfluidic paper-based analytical devices, *Lab Chip*, 2012, 12, 274-280.
77. J. S. Yoon, J. T. Germaine and P. J. Culligan, Visualization of particle behavior within a porous medium: Mechanisms for particle filtration and retardation during downward transport, *Water Resources Research*, 2006, 42.
78. X.-B. Zhang, Z.-Q. Wu, K. Wang, J. Zhu, J.-J. Xu, X.-H. Xia and H.-Y. Chen, Gravitational sedimentation induced blood delamination for continuous plasma separation on a microfluidics chip, *Anal Chem*, 2012, 84, 3780-3786.
79. M. Sun, Z. S. Khan and S. A. Vanapalli, Blood plasma separation in a long two-phase plug flowing through disposable tubing, *Lab Chip*, 2012, 12, 5225-5230.
80. J. H. Son, S. H. Lee, S. Hong, S. M. Park, J. Lee, A. M. Dickey and L. P. Lee, Hemolysis-free blood plasma separation, *Lab Chip*, 2014, 14, 2287-2292.
81. A. Samborski, P. Jankowski, J. Wegrzyn, J. A. Michalski, S. Pawlowska, S. Jakiela and P. Garstecki, Blood diagnostics using sedimentation to extract plasma on a fully integrated point-of-care microfluidic system, *Eng Life Sci*, 2015, 15, 333-339.
82. Y.-A. Chen, A. D. King, H.-C. Shih, C.-C. Peng, C.-Y. Wu, W.-H. Liao and Y.-C. Tung, Generation of oxygen gradients in microfluidic devices for cell culture using spatially confined chemical reactions, *Lab Chip*, 2011, 11, 3626-3633.
83. M. D. Brennan, M. L. Rexius-Hall, L. J. Elgass and D. T. Eddington, Oxygen control with microfluidics, *Lab Chip*, 2014, 14, 4305-4318.
84. S. Grist, L. Yu, L. Chrostowski and K. C. Cheung, Microfluidic cell culture systems with integrated sensors for drug screening, *SPIE MOEMS-MEMS*, 2012, 8251, 825103.
85. E. Leclerc, Y. Sakai and T. Fujii, Microfluidic PDMS (polydimethylsiloxane) bioreactor for large-scale culture of hepatocytes, *Biotechnol Prog*, 2004, 20, 750-755.
86. M. Polinkovsky, E. Gutierrez, A. Levchenko and A. Groisman, Fine temporal control of the medium gas content and acidity and on-chip generation of series of oxygen concentrations for cell cultures, *Lab Chip*, 2009, 9, 1073-1084.
87. S. C. Oppegard, K. H. Nam, J. R. Carr, S. C. Skaalure and D. T. Eddington, Modulating temporal and spatial oxygenation over adherent cellular cultures, *PLoS One*, 2009, 4, e6891.
88. J. F. Lo, E. Sinkala and D. T. Eddington, Oxygen gradients for open well cellular cultures via microfluidic substrates, *Lab Chip*, 2010, 10, 2394-2401.
89. D. K. Wood, A. Soriano, L. Mahadevan, J. M. Higgins and S. N. Bhatia, A biophysical indicator of vaso-occlusive risk in sickle cell disease, *Sci Transl Med*, 2012, 4, 123ra126.
90. P. Vulto, S. Podszun, P. Meyer, C. Hermann, A. Manz and G. A. Urban, Phaseguides: a paradigm shift in microfluidic priming and emptying, *Lab Chip*, 2011, 11, 1596-1602.
91. A. Oskooei, M. Abolhasani and A. Gunther, Bubble gate for in-plane flow control, *Lab Chip*, 2013, 13, 2519-2527.
92. K. Khoshmanesh, A. Almansouri, H. Albloushi, P. Yi, R. Soffe and K. Kalantar-zadeh, A multi-functional bubble-based microfluidic system, *Sci Rep*, 2015, 5, 9942.
93. C. Lochovsky, S. Yasotharan and A. Gunther, Bubbles no more: in-plane trapping and removal of bubbles in microfluidic devices, *Lab Chip*, 2012, 12, 595-601.
94. A. Oskooei and A. Gunther, Bubble pump: scalable strategy for in-plane liquid routing, *Lab Chip*, 2015, 15, 2842-2853.
95. W. Wu, K. T. L. Trinh and N. Y. Lee, Hand-held syringe as a portable plastic pump for on-chip continuous-flow PCR: miniaturization of sample injection device, *Analyst*, 2012, 137, 983-990.
96. P. K. Yuen, H. Su, V. N. Goral and K. A. Fink, Three-dimensional interconnected microporous poly(dimethylsiloxane) microfluidic devices, *Lab Chip*, 2011, 11, 1541-1544.
97. V. N. Goral, S. H. Au, R. A. Faris and P. K. Yuen, Microstructured multi-well plate for three-dimensional packed cell seeding and hepatocyte cell culture, *Biomicrofluidics*, 2014, 8, 046502.
98. K. J. Cha and D. S. Kim, A portable pressure pump for microfluidic lab-on-a-chip systems using a porous polydimethylsiloxane (PDMS) sponge, *Biomed Microdevices*, 2011, 13, 877-883.
99. G. Maier, Gas separation by polymer membranes: beyond the border, *Angew Chem Int Ed Engl*, 2013, 52, 4982-4984.
100. M. Nour, K. Berean, M. J. Griffin, G. I. Matthews, M. Bhaskaran, S. Sriram and K. Kalantar-Zadeh, Nanocomposite carbon-PDMS membranes for gas separation, *Sensors and Actuators B: Chemical*, 2012, 161, 982-988.
101. M. Nour, K. Berean, S. Balendhran, J. Z. Ou, J. Du Plessis, C. McSweeney, M. Bhaskaran, S. Sriram and K. Kalantar-zadeh, CNT/PDMS composite membranes for H2 and CH4 gas separation, *International Journal of Hydrogen Energy*, 2013, 38, 10494-10501.
102. Q. Tian, Q. Song, Y. Xu, Q. Zhu, B. Yu, W. Jin, Q. Jin and Y. Mu, A localized temporary negative pressure assisted microfluidic device for detecting keratin 19 in A549 lung carcinoma cells with digital PCR, *Analytical Methods*, 2015, 7, 2006-2011.
103. Y.-H. Shin, J. Z. Barnett, E. Song, M. T. Gutierrez-Wing, K. A. Rusch and J.-W. Choi, A portable fluorescent sensor for on-site detection of microalgae, *Microelectronic Engineering*, 2015, 144, 6-11.
104. K. Y. Weng, N. J. Chou and J. W. Cheng, Triggering vacuum capillaries for pneumatic pumping and metering liquids in point-of-care immunoassays, *Lab Chip*, 2008, 8, 1216-1219.

105. C. C. Hong and J. C. Chen, Pre-programmable polymer transformers as on-chip microfluidic vacuum generators, *Microfluidics Nanofluidics*, 2011, 11, 385-393.
106. J. N. Lee, C. Park and G. M. Whitesides, Solvent compatibility of poly(dimethylsiloxane)-based microfluidic devices, *Anal Chem*, 2003, 75, 6544-6554.
107. N. Ziane, M. Guirardel, J. Leng and J. B. Salmon, Drying with no concentration gradient in large microfluidic droplets, *Soft Matter*, 2015, 11, 3637-3642.
108. J. Clausell-Tormos, D. Lieber, J. C. Baret, A. El-Harrak, O. J. Miller, L. Frenz, J. Blouwolff, K. J. Humphry, S. Koster, H. Duan, C. Holtze, D. A. Weitz, A. D. Griffiths and C. A. Merten, Droplet-based microfluidic platforms for the encapsulation and screening of Mammalian cells and multicellular organisms, *Chem Biol*, 2008, 15, 427-437.
109. B. Zheng, L. S. Roach and R. F. Ismagilov, Screening of protein crystallization conditions on a microfluidic chip using nanoliter-size droplets, *J Am Chem Soc*, 2003, 125, 11170-11171.
110. Y. S. Shin, K. Cho, S. H. Lim, S. Chung, S. J. Park, C. Chung, D. C. Han and J. K. Chang, PDMS-based micro PCR chip with parylene coating, *Journal of Micromechanics and Microengineering*, 2003, 13, 768-774.